RAMReS Sciences des Structures et de la Matière Vol. 9, N°2 (2025) 242 - 262
http://publication.lecames.org/index.php/mat ISSN: 2630-1180

Ductile fracture models and an Abaqus subroutine for simulating deep drawing damage and predicting part fracture

Dinh Van Tran[1], Chu Van Truong[2,3,*]

[1]*Department of Mechanical Engineering, East Asia University of Technology, 62D/5 Hoang Quoc Viet Str., Hanoi, Vietnam*
[2]*Swiss Information and Management Institute, 6340, 7 Blegistrasse Str., Baar, Switzerland*
[3]*Asia Metropolitan University, 81750, 6, Jalan Lembah Str., Johor Bahru, Malaysia*

Received: 26 August 2025 / Received in revised form: 28 November 2025 / Accepted: 20 December 2025

***Abstract*:**

This study investigates ductile fracture modelling approaches with the objective of identifying a reliable criterion for the numerical simulation of deep drawing processes. A comparative analysis was conducted to evaluate the ability of representative fracture formulations to capture damage evolution under conditions of large plastic deformation. The results indicate that a stress-based damage criterion provides superior predictive capability for fracture initiation compared to conventional strain-based approaches. This model enables a more accurate description of damage accumulation by accounting for the combined effects of stress state and plastic deformation. To facilitate practical application, the selected fracture criterion was implemented in the Abaqus finite element framework through a dedicated user-defined material subroutine (UMAT). The numerical simulations demonstrate that the proposed implementation accurately predicts damage localization and fracture onset at different stages of the forming process. The findings confirm the suitability of the proposed modelling strategy for analyzing deep drawing operations and highlight its potential for improving the reliability of numerical predictions in sheet metal forming. The developed approach provides a practical tool for process optimization and quality improvement in forming applications where accurate fracture prediction is critical.

***Keywords*:** Ductile fracture; Deep drawing; Brozzo criterion; Damage accumulation; Abaqus UMAT.

1. Introduction

Ductile fracture is a complex mechanism that defines the serviceability limits of metallic materials subjected to plastic deformation. Deep drawing, one of the most

* Corresponding author:
Email address: *vantruongchu065@gmail.com (C.V. Truong)*
https://doi.org/10.70974/mat09225242

widely applied sheet-metal forming processes, involves severe plastic deformation along with contact interactions between the sheet, punch, and die. These interactions generate a highly non-uniform stress–strain state, including pronounced through-thickness gradients, evolving stress triaxiality, and non-proportional loading paths. Under such conditions, damage tends to accumulate locally, particularly in the die-radius and wall regions, ultimately leading to fracture.

Although numerous ductile fracture models have been proposed, many demonstrate limited predictive capability under deep-drawing conditions. Phenomenological criteria calibrated under simple loading paths often fail to capture the combined influence of hydrostatic stress, changing stress states, and deformation path dependency inherent to deep drawing. Models that neglect the progressive accumulation of damage or assume proportional loading may provide acceptable predictions for uniaxial tension or simple forming operations, yet they lose accuracy when applied to the complex, contact-dominated, and highly constrained deformation characteristic of deep drawing. Conversely, micromechanical models capable of describing damage evolution frequently require extensive parameter calibration and remain difficult to implement efficiently in large-scale numerical simulations of industrial forming processes.

Consequently, the absence of a universally applicable and computationally efficient fracture model tailored to deep-drawing conditions constitutes a significant scientific and practical challenge. This necessitates a systematic analysis of existing ductile fracture models, with particular emphasis on their ability to represent damage accumulation under non-uniform, multiaxial, and non-proportional loading. Identifying the model that most accurately reflects these mechanisms and developing an appropriate numerical implementation are therefore essential steps toward reliable prediction of material failure during deep drawing and the optimization of forming processes.

For instance, Giang *et al.* [1] studied the deep drawing process of cup-shaped parts made of SUS304 stainless steel using numerical modeling and experimental verification. The authors determined that the use of the Barlat 89 plasticity model allows for accurate prediction of earing formation, which is important for predicting defects during the drawing process. Hà *et al.* [2] investigated the elastic deformation and springback of U-shaped structures produced by deep drawing of copper alloys using numerical modeling and experimental data. They applied the finite element method with the von Mises plasticity criterion and isotropic hardening to analyze the loads and elastic response, which helped to explain the differences in the behavior of different alloys. In addition, Thành [3] proposed an improved phase-field method for predicting crack formation and development in brittle materials, which allows for high accuracy in determining the critical load. The numerical results for seven test structures showed a maximum error of 4.5% compared to reference methods, confirming the effectiveness of the approach for fracture modeling.

Laboubi *et al.* [4] implemented Abaqus numerical modeling of the DC04 steel deep drawing process using a Vectorised User Material (VUMAT) subroutine to predict ductile fracture, showing high agreement with experimental data. Zhu *et al.* [5] performed numerical simulations in Abaqus of the fracture process of high-strength X80 pipe steel using VUMAT to implement the DF2014 ductile fracture criterion, which allowed them to accurately predict crack trajectories under various stress states. Dey and Kiran [6] demonstrated numerical modeling in Abaqus to generate training data and implement the Gurson–Tvergaard–Needleman ductile fracture model, after which they used a long short-term memory (LSTM) neural network to predict the load–compression behavior before fracture in metal samples. In turn, Talebi-Ghadikolaee *et al.* [7] implemented the normalized Cockroft–Latham criterion in Abaqus/Explicit through a custom subroutine to predict the flexural failure

of AA6061-T6, confirming the accuracy of numerical modeling with an error of 2.57% and using machine learning to improve the prediction of damage evolution.

Talebi-Ghadikolaee *et al.* [8] implemented three ductile fracture criteria (Ayada, Rice–Tracey, and normalized Cockcroft–Latham) in Abaqus/Explicit via a custom subroutine to predict fracture in AA6061-T6 during roll forming. Their study focused on selecting the most accurate criterion through calibration using a flat tensile test, with the Ayada model providing the lowest error. In contrast, the present work does not aim at criterion comparison for a specific alloy or forming operation, but rather at identifying and implementing a fracture model that explicitly captures damage accumulation under the complex stress states characteristic of deep drawing.

Wang *et al.* [9] developed a ductile fracture model incorporating both stress triaxiality and the Lode angle parameter, which was implemented in Abaqus/Explicit using VUMAT and validated for Ti-6Al-4V under controlled, predefined stress states. While their approach emphasizes the accurate reproduction of fracture displacement and crack morphology across different loading paths, it is primarily oriented towards general fracture characterization rather than process-specific forming operations. By contrast, the current study focuses on a forming-oriented implementation, targeting the prediction of failure initiation during deep drawing through a damage accumulation framework. Similarly, Guo *et al.* [10] proposed a damage-adjusted viscoplasticity model for aluminum alloys under hot deformation, explicitly accounting for temperature and strain-rate effects and implementing the formulation through VUMAT. Their work addresses thermomechanical conditions typical of hot forming, whereas the present study concentrates on cold deep-drawing conditions and prioritizes the representation of damage evolution driven by multiaxial stress states and non-uniform plastic deformation.

This study aims to compare ductile fracture models and determine the most effective one for modeling the deep drawing process, which has not been comprehensively addressed in the literature. The tasks include analysis of existing models, development of a specialized subroutine, and numerical modeling of the process.

2. Materials and methods

To achieve the research goals, the study was conducted in three main phases: (1) a systematic review and comparative analysis of existing ductile fracture models, (2) the development of a specialized Abaqus user subroutine (UMAT) implementing the selected fracture criterion, and (3) numerical implementation and validation through theoretical simulation of a deep-drawing process.

2.1. Review and selection of ductile fracture models

During the initial phase, the principal ductile fracture models (including Cockcroft & Latham, Brozzo, Oh, Johnson & Cook, Bai & Wierzbicki, Modified Mohr-Coulomb, Lou-Huh, Gurson-Tvergaard-Needleman, and Lemaitre) were analyzed with respect to their underlying assumptions, input parameter requirements, sensitivity to stress triaxiality, ability to account for damage accumulation, and applicability under the non-uniform, non-proportional loading conditions characteristic of deep drawing.

Models that neglect hydrostatic stress effects or assume simple proportional loading paths were identified as less suitable for deep-drawing simulations. In contrast, criteria explicitly incorporating stress triaxiality and cumulative damage were found to be more appropriate. Schematic formulations for fracture prediction using the Cockcroft & Latham, Brozzo, and Oh models were examined in detail. Based on this analysis, the Brozzo model was selected as the most suitable framework due to its proven capability to capture progressive damage accumulation under multiaxial stress states typical of sheet metal forming operations like deep drawing.

2.2. Development of the Brozzo-based UMAT subroutine

The second phase involved creating a specialized custom UMAT subroutine implementing the Brozzo fracture criterion. This selection was based on the model's ability to accurately account for damage accumulation in materials undergoing large plastic deformation, which is critical for simulating deep drawing.

The fundamental equation of the integral fracture criterion, describing damage accumulation through the integration of the ratio of maximum principal stress to equivalent stress over plastic strain, was defined as:

$$\int_0^{\varepsilon_f} \left(\frac{\sigma_1}{\sigma_e}\right) d\varepsilon_p = C \tag{1}$$

where σ_1 is the maximum principal stress, σ_e is the von Mises equivalent stress, $d\varepsilon_p$ is the incremental plastic strain, and C is a material-dependent parameter.

The implementation of the fracture criterion and the associated plastic flow algorithm was carried out within the Abaqus 2024 computational environment. Key interface elements utilized in the simulation setup included:

- **Parts:** Geometry creation for the sheet metal blank
- **Material:** Definition of mechanical properties including the plasticity model
- **Section:** Assignment of material type and distribution across the part
- **Step:** Configuration of analysis steps and solution procedures
- **Instance:** Creation of geometry instances for model assembly
- **Boundary Condition:** Application of constraints and loading conditions
- **Global Seeds:** Specification of finite element mesh parameters for numerical computation

The subroutine algorithm was designed to calculate key deformation state parameters, determine damage accumulation, and update material state variables at each integration point and time increment.

2.3. UMAT programming and numerical implementation

The final phase involved programming the User Material (UMAT) subroutine in Fortran based on the Brozzo fracture criterion. The code structure was designed to incorporate damage accumulation at each finite element node through incremental updates of a state variable. The damage criterion for the Brozzo model, determining material failure initiation, was implemented as:

$$D = \frac{\sigma_{\max}}{\sigma_f} + \varepsilon_p \tag{2}$$

where σ_f is the material's ultimate tensile strength, $\sigma_{\max}$ is the maximum principal stress, and ε_p is the accumulated equivalent plastic strain. Material failure is assumed to occur when $D \geq 1$.

To characterize material plastic flow, the anisotropic Hill48 yield function was employed, accounting for directional dependence of mechanical properties:

$$\overline{\sigma}_H = \sqrt{\begin{aligned} &F(\sigma_{yy}-\sigma_{zz})^2 + G(\sigma_{zz}-\sigma_{xx})^2 \\ &+ H(\sigma_{xx}-\sigma_{yy})^2 + 2L\tau_{yz}^2 \\ &+ 2M\tau_{zx}^2 + 2N\tau_{xy}^2 \end{aligned}} \tag{3}$$

where $\sigma_{xx}, \sigma_{yy}, \sigma_{zz}$ are normal stress components, $\tau_{xy}, \tau_{yz}, \tau_{zx}$ are shear stress components, and F, G, H, L, M, N are material coefficients characterizing anisotropic plastic response.

2.4. Numerical modeling and validation framework

Theoretical numerical modeling of the deep drawing process was conducted using the implemented fracture criterion under realistic sheet material deformation conditions. Special emphasis was placed on identifying

regions of damage concentration and predicting the onset of part failure at different deformation stages.

To verify the robustness of the Brozzo-based UMAT implementation, a sensitivity analysis was performed considering mesh density, through-thickness integration points, time increment size, and key material parameters. Variations in these inputs resulted in changes of less than 5% in predicted fracture initiation strain and did not significantly affect damage localization patterns, confirming the numerical stability of the implemented model.

3. Results and discussion

3.1. Comparative analysis of ductile fracture models

Ductile fracture constitutes a critical aspect of metallic material deformation mechanics, particularly in processes involving substantial plastic deformation such as deep drawing. The selection of an appropriate fracture model is essential for accurately predicting crack initiation and propagation, which enables defect prevention in finished products and optimization of manufacturing processes. Various ductile fracture models describe damage mechanisms through different approaches, ranging from phenomenological to micromechanical frameworks [11–13].

The Cockcroft & Latham model represents a phenomenological approach developed to predict ductile fracture during plastic deformation [13, 14]. This model assumes that material failure occurs when the integrated value of the maximum principal stress exceeds a critical threshold, calculated as the integral of maximum principal stress over the plastic deformation history. While widely employed to assess crack resistance in high-grade steels undergoing significant plastic deformation, this model exhibits limitations for deep-drawing applications due to its neglect of hydrostatic stress effects.

The Brozzo model constitutes an enhancement of the Cockcroft & Latham framework [15, 16], incorporating the influence of hydrostatic stress—a critical factor for processes characterized by high triaxial stresses. By combining maximum principal stress criteria with a hydrostatic component, the Brozzo model provides more accurate failure predictions under conditions of elevated triaxial stress, as commonly encountered in forming operations like deep drawing and extrusion. For metal forming processes involving substantial hydrostatic stress levels, the Brozzo model delivers superior prediction accuracy for materials such as aluminum alloys, extensively utilized in aerospace and automotive industries [17–19].

As illustrated in Table 1, the Brozzo model estimation process involves calculating principal and hydrostatic stresses, combining these measures, and integrating them with plastic strain to determine when stress levels exceed critical values. This approach demonstrates better correlation with experimental data compared to models considering only maximum principal stress.

The Oh model represents a specialized framework for predicting material failure in axisymmetric extrusion processes where stress state control is paramount [20, 21]. While based on maximum principal stress, this model incorporates specific characteristics of spatial stress distribution typical of extrusion operations, where materials experience significant loading under constrained deformation conditions. This model effectively assesses defect formation and failure risk during metal extrusion processes, such as aluminum profile or copper wire production, where stress states evolve along the process axis.

The Johnson & Cook model provides an important tool for predicting material failure under high-speed, elevated-temperature deformation conditions, such as impact or explosive loading scenarios [22, 23]. This model incorporates not only mechanical material characteristics but also temperature effects and strain rate influences, making it particularly valuable for analyzing material behavior under extreme conditions encountered in aerospace or defense applications.

Table 1
Conceptual comparison of ductile fracture prediction schemes.

Aspect	Cockcroft & Latham model	Brozzo model	Oh model
Initial loading stage	External load leading to plastic deformation	External load leading to plastic deformation	External load leading to plastic deformation
Primary stress evaluation	Calculation of principal stresses	Calculation of principal stresses	Calculation of principal stresses
Governing stress parameter	Maximum principal stress, $\sigma_{\max}$	Maximum principal stress, $\sigma_{\max}$, combined with hydrostatic stress	Maximum principal stress, $\sigma_{\max}$, modified by a correction factor
Additional stress component	Not considered	Hydrostatic stress, σ_h	Stress-state correction factor accounting for confined deformation
Stress combination strategy	Direct use of $\sigma_{\max}$	Combination of $\sigma_{\max}$ and σ_h	Combination of $\sigma_{\max}$ and correction factor
Damage accumulation measure	Integration of $\sigma_{\max}$ over plastic strain	Integration of combined stress measure over plastic strain	Integration of corrected stress measure over plastic strain
Integral form	$\int f(\sigma_{\max})d\varepsilon_p$	$\int f(\sigma_{\max}, \sigma_h)d\varepsilon_p$	$\int(\sigma_{\max} \times \text{correction})d\varepsilon_p$
Fracture criterion	Comparison with critical value C	Comparison with critical value C	Comparison with critical value C
Failure condition	$\sigma_{\max} > C$	Combined stress measure $> C$	Corrected stress measure $> C$
Predicted outcome	Moment of fracture initiation	Moment of fracture initiation	Moment of fracture initiation
Suitability for deep drawing	Limited (no hydrostatic stress effect)	High (accounts for triaxial stress state)	Moderate (specialized for confined stress conditions)

Other models offer utility in specific fracture prediction contexts. The Bai & Wierzbicki micromechanical model includes a Lode angle parameter describing principal stress equilibrium and triaxial stress effects, making it applicable for crack development prediction in processes where these factors dominate, such as deep drawing or extrusion. The Modified Mohr-Coulomb model finds widespread use in predicting ductile fracture during metal forming operations, considering both plastic strain and hydrostatic stress to effectively model complex loading typical of deep drawing processes. The Lou-Huh micromechanical model, based on micropore growth and coalescence mechanisms, provides accurate ductile fracture predictions for low- to medium-strength metals undergoing large plastic strains.

The Gurson-Tvergaard-Needleman model enjoys popularity for its approach to modeling ductile fracture through evolving material porosity during deformation, enabling detailed description of metal dam-

age in processes like drawing [24–26]. The Lemaitre model, also founded on damage micromechanics, considers pore development and micropore-crack interactions, proving useful for describing ductile fracture in materials experiencing substantial plastic deformation [27].

Table 2 presents a comprehensive comparison of these ductile fracture models regarding their principal advantages and limitations. The selection of an appropriate ductile fracture model for deep drawing applications depends on specific process characteristics and material properties. While each model offers particular advantages under specific loading and strain conditions, their inherent limitations necessitate careful selection based on production process specifics. For deep-drawing operations where high triaxial stresses play a dominant role, the Brozzo model emerges as particularly suitable. Its incorporation of hydrostatic stress effects enables more accurate prediction of material failure, justifying the development of an Abaqus subroutine based on this model.

3.2. Development and implementation of the Brozzo-based Abaqus subroutine

The Brozzo model employs a criterion incorporating maximum principal stress state and equivalent plastic strain to estimate failure initiation (Equation 1). This formulation proves particularly suitable for sheet metals undergoing deep drawing. For Abaqus implementation, the simulation environment was initialized by selecting the Standard/Explicit Model option and creating a new model designated Model-1.

Table 2
Comparison of ductile fracture models.

Model	Advantages	Limitations
Cockcroft & Latham	Straightforward implementation for crack resistance assessment	Neglects hydrostatic stress and triaxial stress effects
Brozzo	Accurate failure prediction under high triaxial stresses	Limited applicability for processes with minimal plastic deformation
Oh	Specialized for axisymmetric extrusion processes	Restricted to axisymmetric operations
Johnson & Cook	Incorporates temperature and strain rate effects at high speeds	Reduced accuracy for low-speed processes
Bai & Wierzbicki	Includes Lode angle parameter for stress equilibrium description	Requires extensive experimental calibration across stress states
Modified Mohr–Coulomb	Capable of modeling complex forming loads	Inconsistent accuracy for low-strength materials
Lou–Huh	Excellent for crack development in low-strength metals	Limited applicability for high-strength materials
Gurson–Tvergaard–Needleman	Detailed damage description through porosity consideration	Not always suitable for high-strength materials
Lemaitre	Accurately describes micropore–crack interactions	Implementation challenges for certain processes

Within the Part module, a deformable component named DeepDrawingPart was created (Fig. 1). The selection of shell elements as the fundamental modeling approach was justified by the workpiece thinness, as shell elements offer greater computational efficiency than volumetric elements for such geometries, reducing computational complexity—a critical consideration for large plastic deformation simulations.

Workpiece geometry was defined through a circular sketch centered at coordinates (0,0), corresponding to XY-axis intersection (Fig. 2). The circle diameter was set to 200 mm, representing a standard dimension for deep drawing applications. Circular workpiece geometry ensures uniform stress distribution during deformation, while the thin-sheet approach with planar sketches provides optimal modeling efficiency, with the coordinate system ensuring proper part positioning and constraint application.

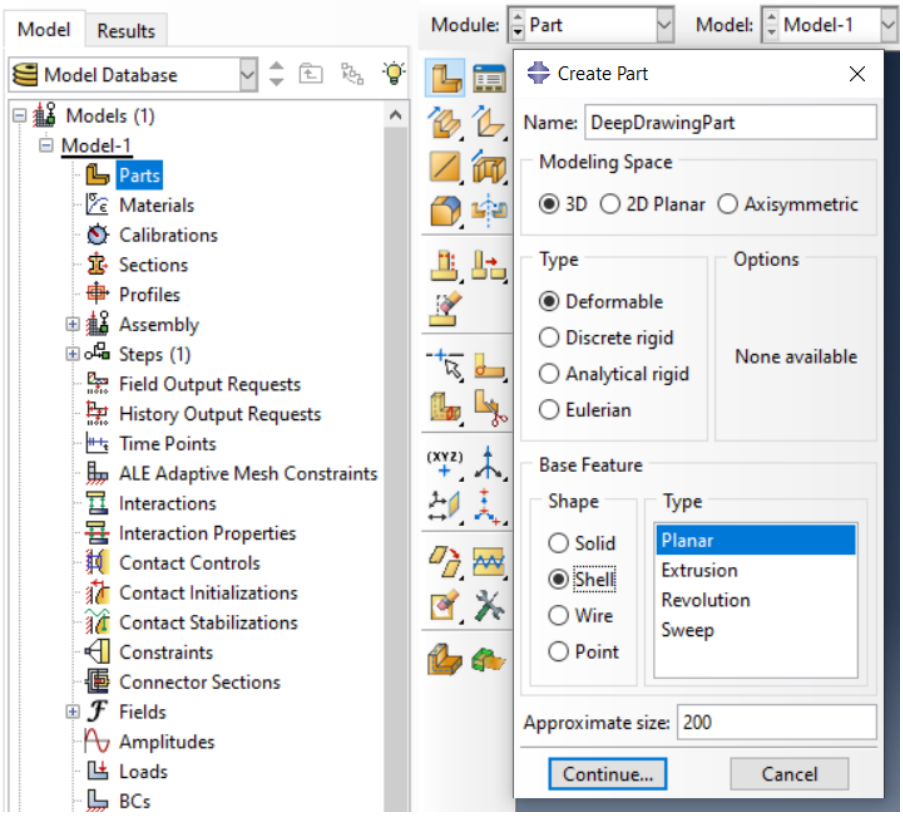

Fig. 1. Creation of a Deep Drawing Part.

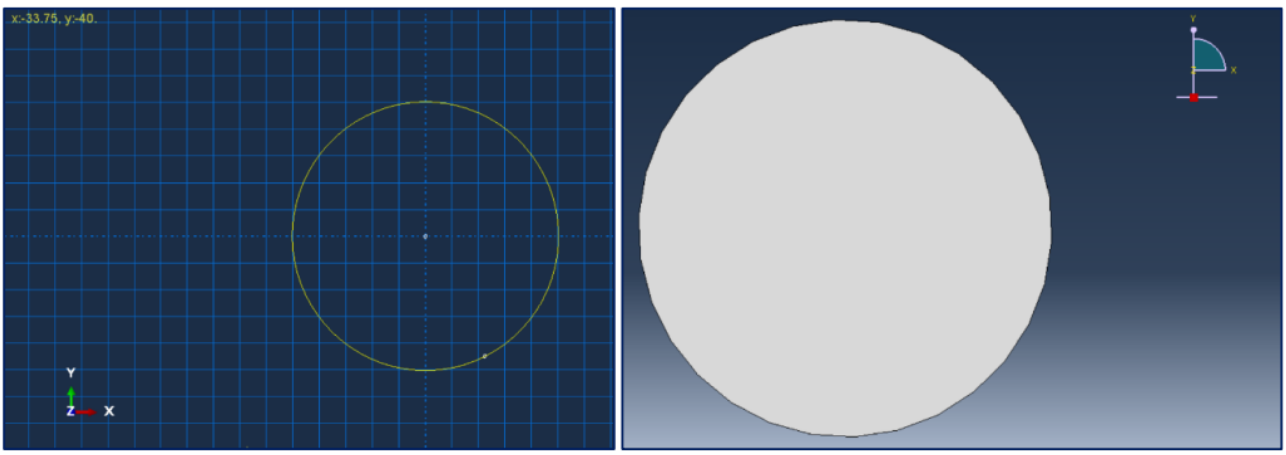

Fig. 2. Creation of a workpiece sketch.

Metal plastic deformation modeling requires definition of elastic and plastic material properties. Elastic characteristics are described by Young's modulus and Poisson's ratio, while yield strength defines plastic deformation onset. Within Abaqus, plasticity is modeled through experimental stress-strain relationships, enabling accurate reproduction of metal behavior during drawing operations.

Accordingly, a material named DeepDrawingMaterial was created (Fig. 3) with Mechanical Elasticity Elastic category and Isotropic type, corresponding to isotropic material properties. Elastic characteristics were defined with Young's modulus of 210,000 MPa and Poisson's ratio of 0.3. To account for significant plastic deformation during deep drawing, material ductility was incorporated through Plasticity Plastic properties, with yield stress defined as a function of plastic strain: 250 MPa at 0.0 strain, 300 MPa at 0.01 strain, and 350 MPa at 0.05 strain.

Shell thickness assignment involved defining a material section for the created part (Fig. 4). Within the Sections module, a DeepDrawingSection was created with Shell category and Homogeneous material type, assuming uniform properties throughout the part. Shell thickness was set to 2 mm, typical for sheet metals in deep drawing applications. The Simpson integration method was selected for thickness integration, providing enhanced accuracy for nonlinear materials undergoing plastic deformation. Five through-thickness integration points were specified, as 5–7 points generally suffice for accurate plastic deformation results. For thin shell modeling, additional integration points improve result accuracy, particularly for large plastic strains, with the Simpson method reducing errors in complex plastic deformation simulations.

Section assignment was performed through the Assign menu (Fig. 5). For the DeepDrawingPart, the previously created DeepDrawingSection was selected and applied to the Set-1 region. The Middle surface parameter was used for thickness definition, representing standard practice for thin-walled shells that correctly accounts for material thickness in deformation analysis. This assignment determines material type and geometry for model components, with average surface thickness assignment enabling accurate material thickness accounting and efficient modeling of sheet deformations occurring primarily in the shell plane.

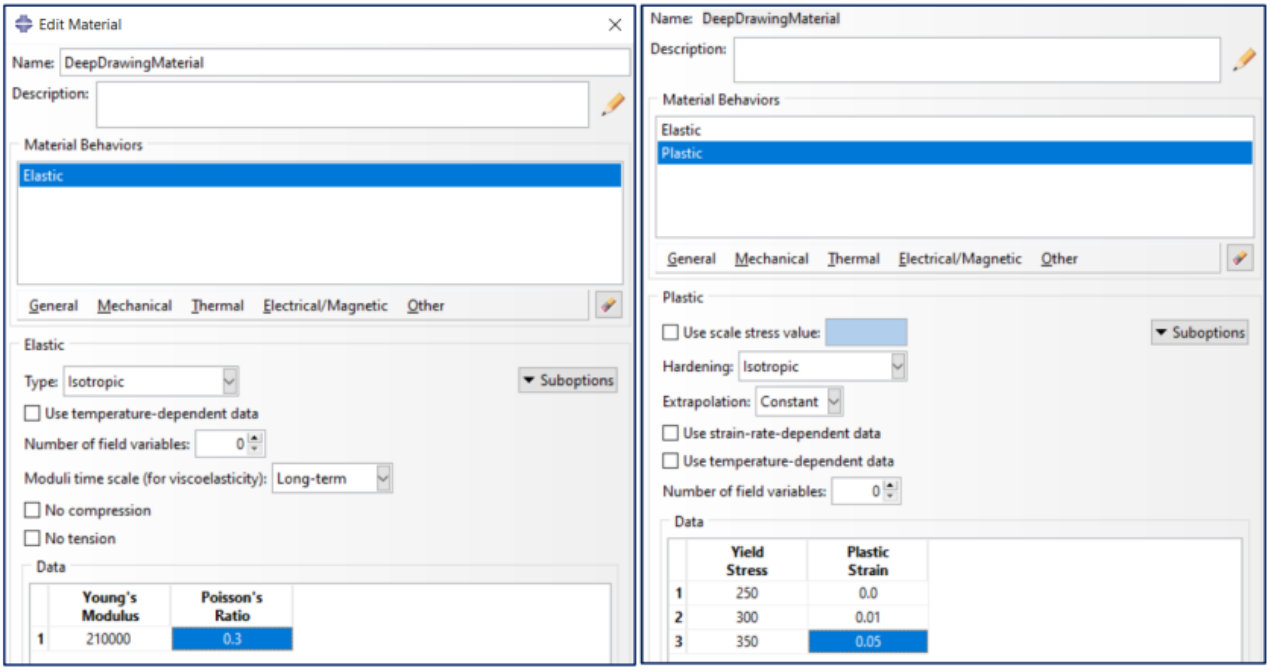

Fig. 3. Material definition.

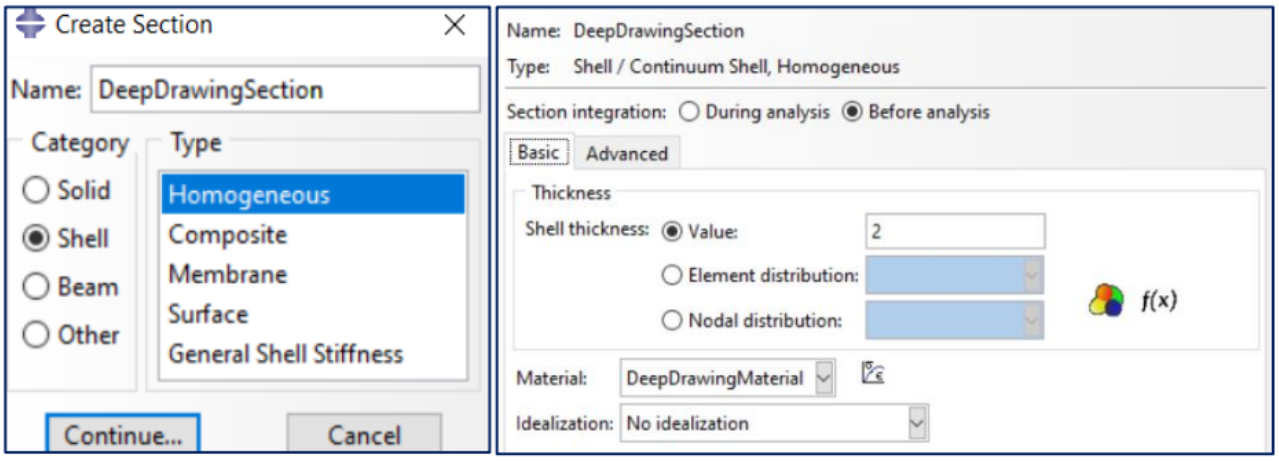

Fig. 4. Shell section properties and thickness integration definition.

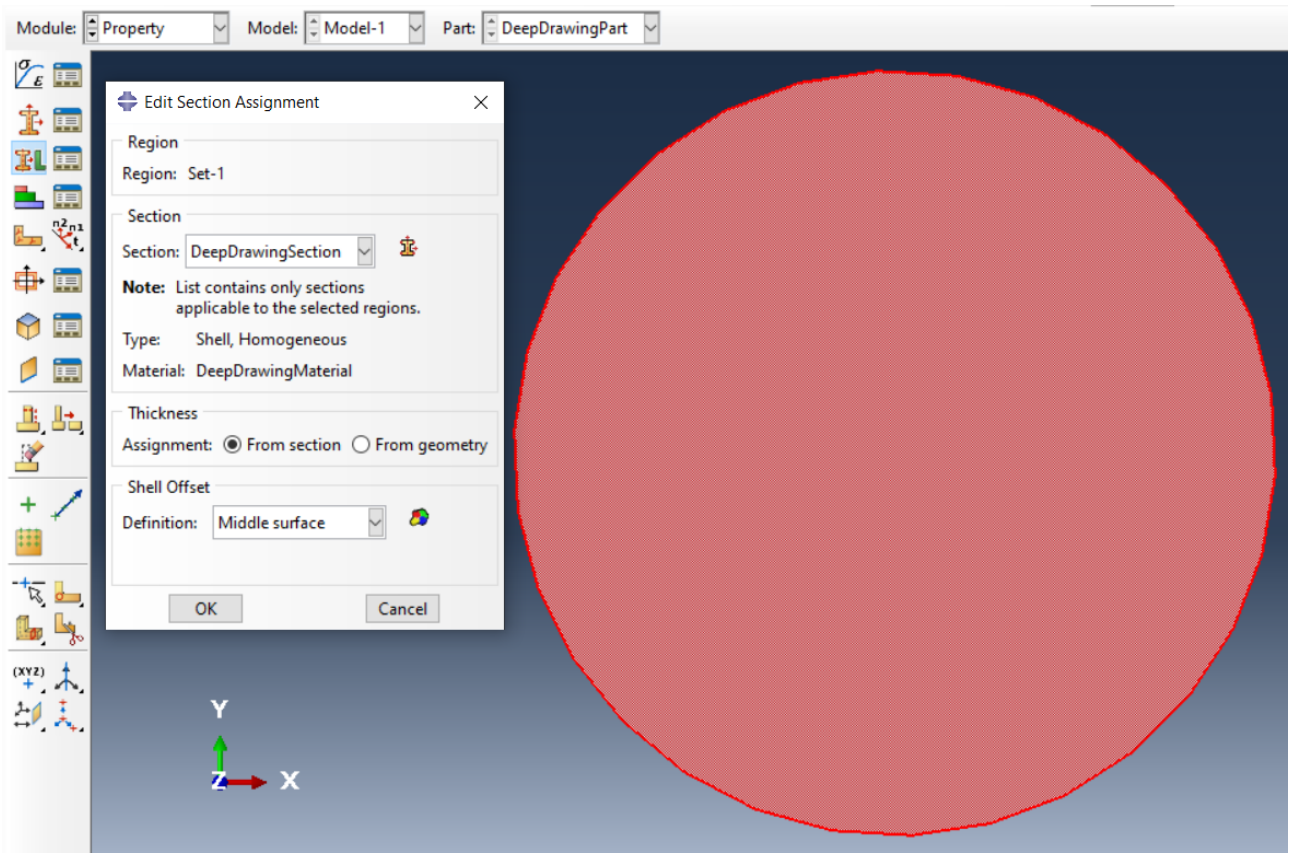

Fig. 5. Section assignment process.

Following geometry creation, material assignment, and shell thickness definition, parts were positioned in space to form the final model geometry (Fig. 6). This was accomplished within the Assembly module using the "Dependent" instance type to create a model instance, establishing the required spatial part configuration for subsequent analysis. Within the Step module, a calculation step defining the modeling stage was created. Since deep drawing constitutes a gradual process, the "Static, General" step type was selected for static load modeling. Step time was set to 1.0, defining total calculation duration. The "Nlgeom" parameter was activated to account for geometric nonlinearity, essential for accurate plastic deformation modeling.

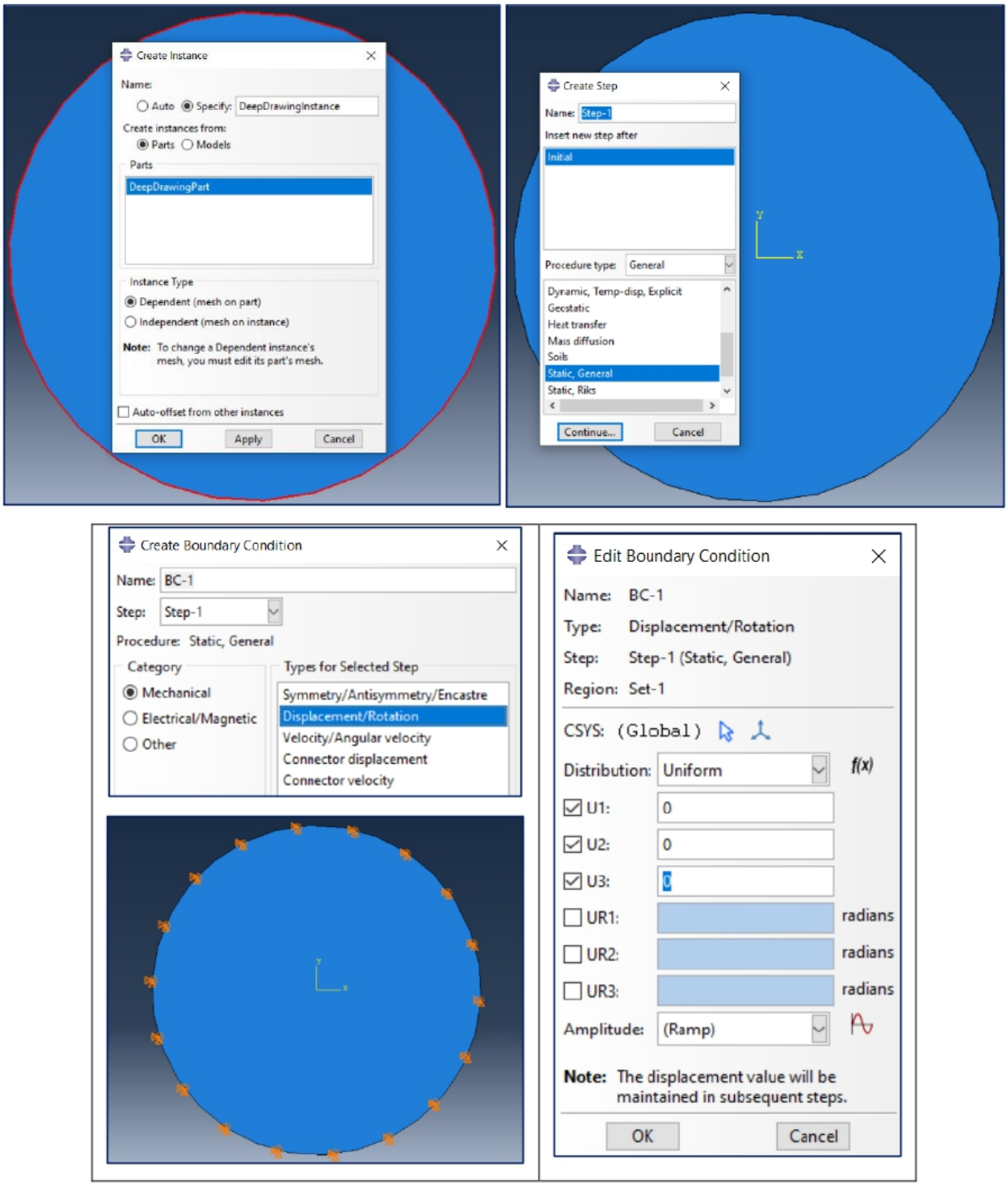

Fig. 6. Assembly, step creation, and boundary condition definition.

Boundary conditions were defined within the Load module (Fig. 6). A Boundary Condition named BC-1 was created within the Step-1 static step, with Mechanical category and Displacement/Rotation type selected for part motion restriction. To fully constrain the part, values U1=0, U2=0, and U3=0 were specified, corresponding to fixation along X (horizontal), Y (vertical), and Z (depth) axes, respectively. This configuration properly represents interaction with other model components or supports during analysis.

Mesh generation for computational analysis was performed within the Mesh module (Fig. 7). The DeepDrawingPart was selected, with mesh density controlled through the Seed Part command determining element

size. An element size of 7 mm was specified, providing optimal balance between deformation modeling accuracy and computational efficiency for deep drawing simulation.

The S4R element type—a four-node shell element with reduced integration—was selected, enabling accurate stress and strain modeling in thin-walled materials while minimizing shear locking effects.

Following mesh generation, the model was prepared for analysis and subsequent subroutine implementation addressing plastic deformation specifics during deep drawing. The implemented subroutine accurately accounts for material damage according to the selected Brozzo model while ensuring proper integration within the Abaqus computational environment.

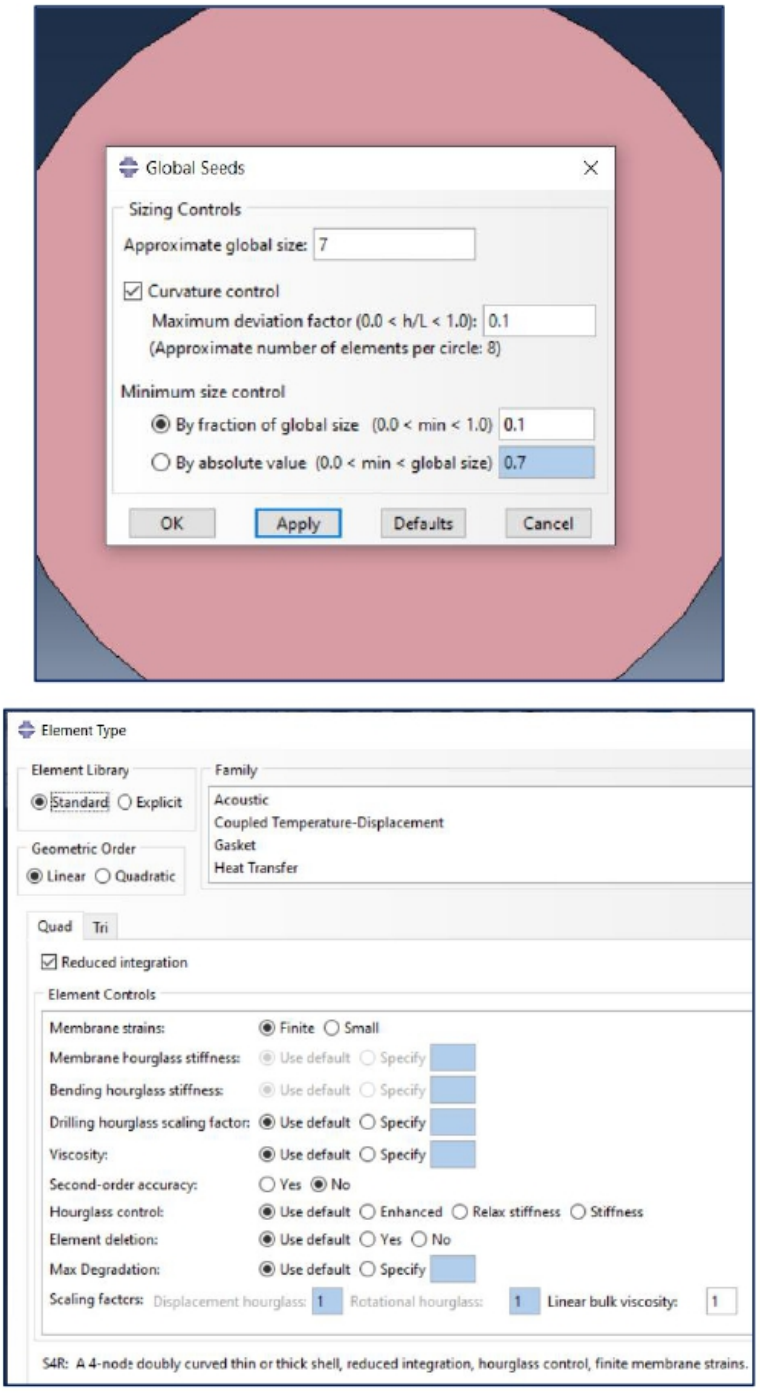

Fig. 7. Mesh generation for the model.

3.3. Subroutine programming and deep drawing process modeling

The Brozzo model foundation rests on a damage criterion combining two principal parameters: maximum normal stress and plastic strain. Material failure occurs when these parameter values exceed critical thresholds (Equation 2). Subroutine programming involves damage calculation based on stress and strain evolution, utilizing these parameters to model damage development during deep drawing (Fig. 8).

The presented UMAT framework translates Brozzo-type damage logic into an incremental, element-wise update procedure executed at each material point and time increment. Argument lists stress(6), statev(*), and props(*) provide essential interfaces between Abaqus and the constitutive routine: stress(6) contains current Cauchy stress components in Voigt notation, statev(*) stores history-dependent variables (e.g., accumulated plastic strain and damage measure), and props(*) supplies user-defined material constants (yield-stress scale and plastic-strain threshold).

```
subroutine umat(stress, statev, ddsdde, sse, spd, scd, rpl, dtime, temp,
     1   dtemp, predef, dpred, nstatev, props, nprops,
     2   coords, drot, pnewdt, celent, time, dtime,
     3   plast, temperature)
c
      implicit none
      real(8) :: stress(6), statev(*), ddsdde(6,6), sse, spd, scd, rpl
      real(8) :: dtime, temp, dtemp, predef(*), dpred(*)
      integer :: nstatev, nprops
      real(8) :: props(*), coords(3), drot(3,3)
      real(8) :: pnewdt, celent, time(2), plast
      real(8) :: temperature
c
      ! Initialization for the Brozzo model parameters
      real(8) :: sigma_max, epsilon_p, damage_criteria, damage
      real(8) :: yield_stress, strain_threshold
c
      ! Define critical parameters (adjust values as needed)
      yield_stress = props(1)        ! Yield stress
      strain_threshold = props(2)    ! Plastic strain threshold

      ! Calculate damage based on strain and stress
      sigma_max = maxval(stress)     ! Maximum stress
      epsilon_p = statev(1)          ! Plastic strain state

      ! Damage criterion check (Brozzo's model)
      damage_criteria = sigma_max / yield_stress + epsilon_p / strain_threshold
      if (damage_criteria > 1.0) then
         ! Apply damage to material
         damage = 1.0
      else
         damage = damage_criteria
      end if

      ! Update stress with damage
      stress = stress * (1.0 - damage)

      ! Store damage in the state variable for future steps
      statev(1) = damage
c
      return
end subroutine umat
```

Fig. 8. Example of subroutine code structure.

Following variable initialization, the routine extracts a scalar driving stress measure (sigma_max) from the stress tensor—representing maximum principal/normal stress governing void growth and coalescence in the Brozzo framework—and reads accumulated plastic strain (epsilon_p) from state variables, providing deformation history required for cumulative damage assessment.

The subsequent code block defines the damage indicator damage_criteria as a normalized combination of the stress driving term and plastic straining, thereby mapping the Brozzo concept (failure driven by tensile stress under plastic flow) into a computationally efficient scalar measure evaluated incrementally. The conditional statement (if (damage_criteria $\geq$ 1.0)) implements fracture onset by saturating damage at unity once critical levels are reached; otherwise, damage evolves proportionally with current criterion values, reflecting progressive degradation. The subsequent stress update, stress = stress * (1.0 - damage), represents a stiffness/strength reduction strategy: as damage accumulates, the routine reduces effective stress-carrying capacity, mimicking load-bearing area loss associated with ductile degradation. Finally, the updated damage variable is written back into statev(1), ensuring history-dependent material response across increments and enabling post-processing of spatial damage localization (e.g., in die-radius and wall regions) during deep drawing.

The UMAT subroutine code was saved in a file named brozzo_umat.f. For Abaqus execution, a material (BrozzoMaterial) was created within the Property module, with basic parameters (Yield Stress and Strain Threshold) specified in the Mechanical User Material tab. Within the Job module, a new calculation process (DeepDrawingJob) was created, with the subroutine file specified in the User Subroutine File field within Job Manager. Calculation execution was initiated through the Submit command, with results visualized within the Visualization module.

Numerical modeling of the UMAT subroutine for the Brozzo criterion was performed in Abaqus using a finite element model of the deep drawing process. This model enables prediction of damage accumulation and assessment of fracture zones in sheet material. The geometric model comprises an axisymmetric plate corresponding to typical drawn workpiece dimensions. The material is represented as an isotropic elastoplastic continuum with damage, with plastic flow described through a linear hardening model. Tool-workpiece contact interactions incorporate friction characterized by a Coulomb friction coefficient. Computational stability was ensured through a rigid-surface approach, with the workpiece modeled using shell finite elements. For dynamic process modeling, an explicit integration algorithm was employed to efficiently simulate large plastic deformations.

During each analysis increment, Abaqus passes the stress tensor to UMAT for maximum principal stress calculation and plastic strain updating, enabling accurate damage accumulation assessment. The damage criterion is defined as the sum of normalized maximum principal stress and accumulated plastic strain, with material damage occurring when this sum exceeds a critical threshold. Following computation completion, damage distribution in contact zones is analyzed, revealing damage localization patterns that predict crack formation and identify regions most susceptible to damage. Table 3 summarizes principal modeling parameters, confirming the UMAT subroutine's effectiveness for implementing the Brozzo criterion in deep drawing simulations while adequately representing physical material fracture processes under deep drawing conditions.

3.4. Discussion and comparative analysis

The present study demonstrates that Brozzo criterion implementation in Abaqus enables accurate prediction of fracture initiation during deep drawing operations. Similar to Jia *et al.* [28], whose phenomeno-

logical model for aluminum alloys showed good accuracy in damage zone identification, the current approach applies the criterion to more complex geometric configurations, extending its applicability range. Overall, the Brozzo criterion facilitates assessment of plastic deformation effects on fracture development. Unlike Zhang *et al.* [29], who employed a probabilistic model for ultimate strain prediction, the current methodology adopts a deterministic approach focused on damage prediction during deep drawing while considering initial porosity effects. Despite methodological differences, both approaches demonstrate consistent accuracy in fracture zone prediction.

Consistent with Tandoğan and Yalcinkaya [30], who utilized Abaqus for numerical fracture modeling, the present investigation employs standard software capabilities combined with a custom subroutine for damage accumulation assessment, rather than custom element development. This implementation incorporates stress-strain state influences on fracture development without introducing additional model components. Unlike Akitarak [31], who employed VUMAT, VUHARD, and VUSDFLD subroutines, the current implementation is based on UMAT, enabling analysis within the Abaqus environment with controlled stress state and damage evolution tracking. Both approaches confirm standard Abaqus functionality extension effectiveness for fracture prediction while employing different numerical strategies.

Current results indicate that ductile fracture models provide accurate failure prediction during deep drawing, correlating with Choi *et al.* [32], who proposed a specialized model for shell elements. While their model focuses on thin-walled structures validated under diverse conditions, both approaches for ductile fracture in various geometries provide high accuracy in damage zone prediction. The current deep drawing model can be enhanced through extended geometric feature analysis, broadening its application potential for diverse engineering challenges.

Table 3
Principal modeling parameters.

Parameter	Value	Description
Model type	Axisymmetric	Incorporates deep drawing process symmetry
Material type	Isotropic elastoplastic	Incorporates plastic hardening and damage
Contact boundary condition	Friction (μ)	Describes workpiece–tool interaction
Time integrator	Implicit (Static, General)	Represents quasi-static deep drawing conditions
Stress state	Stress tensor (σ_{ij})	Determines mechanical condition at each point
Damage criterion	Equation 2	Determines failure initiation
Damage localization	Contact areas	Corresponds to regions of maximum stress and plastic deformation
Modeling result	Failure prediction	Identifies critical regions and material behavior

Khaboushani *et al.* [33] proposed a strain energy-based fracture criterion for deep drawing fracture assessment, demonstrating high accuracy in predicting fractures resulting from high radial stresses in bowl walls. This method incorporates various fracture mechanisms based on strain energy considerations. Compared to the current Brozzo criterion implementation through UMAT, their approach employs different fracture prediction methodology. Despite methodological distinctions, both approaches demonstrate high accuracy in predicting failure initiation during deep drawing.

Current results demonstrate high accuracy in predicting deep drawing failure using ductile fracture models in Abaqus, consistent with Ben Said *et al.* [34], who developed a mathematical model for crack formation prediction during deep drawing using anisotropic plasticity equations and custom Abaqus subroutines. Both studies employ UMAT, confirming modeling effectiveness. Alternatively, Clayton [35] proposed a method for shear strain and phase transition estimation during fracture. While focusing on different fracture mechanisms, this approach also demonstrates high accuracy in failure prediction. Thus, both study results are consistent, confirming numerical model effectiveness for failure prediction despite different mechanism emphases.

Similar to Van den Abeele [36], who analyzed GTN model application for detailed ductile fracture modeling through evolving material porosity during deformation, the current study addresses simpler approaches reducing implementation complexity in industrial settings. Hosseini Mansoub *et al.* [37] employed three-axis stress state and damage functions for failure location prediction, analogous to the current approach. However, their study utilizes UMAT for model linkage to Stress Forming Limit Diagrams (SFLD), while the current implementation applies UMAT for direct Brozzo model failure criterion implementation, enabling direct consideration of damage accumulation during material deformation in deep drawing.

Compared to Ma *et al.* [38], who employed a phase-field model with energy approach for shell structure ductile fracture prediction, the current study analyzes Brozzo model capabilities for material failure prediction during deep drawing, addressing damage accumulation from plastic deformation. Study results are consistent regarding plastic deformation consideration but differ in methodological approaches. Regarding Basak and Panda [39], who utilized the Bai & Wierzbicki model for aluminum alloy fracture limit prediction, the current study also considers this model important for crack prediction, particularly in processes like deep drawing, but emphasizes the Brozzo model. Results are consistent in recognizing the Bai & Wierzbicki model as a micromechanical framework incorporating Lode angle parameters and triaxial stress, proving useful in high-cracking-rate processes.

Current results demonstrate the importance of model application for deep drawing failure prediction, similar to Ganjiani [40], who presented a triaxial stress-incorporating model. However, their study employed VUMAT in Abaqus/Explicit, while the current work utilizes UMAT for deterministic prediction. Consistent with Wu and Lou [41], whose DF2016 model demonstrated high accuracy considering strain trajectories, the current model also shows high accuracy levels, particularly in deep drawing contexts. Both approaches demonstrate model effectiveness for fracture prediction, though the current study focuses on specific deformation processes.

Current Brozzo-based results exhibit certain distinctions compared to Fagerhøi and Bergsbakken [42], who analyzed Concrete Damaged Plasticity model parameters for concrete in Abaqus. While both studies address material failure modeling, the current approach aims to predict failure during deep drawing, while their study analyzes parameter change effects on modeling accuracy. Despite material and application differences, both studies confirm that frac-

ture prediction accuracy depends on proper model parameter configuration and its ability to adequately represent material behavior under diverse loading conditions.

Current conclusions estimate failure timing and location through stress and strain integration. Similarly, Aksen *et al.* [43] employed ductile damage functions for dual-phase steels and combined plasticity models for fracture initiation assessment. Common features include emphasis on fracture location prediction accuracy, though current results focus on specific deep drawing processes while their work considers different deformation conditions and material types. Additionally, the current study analyzes damage accumulation, while Park *et al.* [44] utilize the Hosford-Coulomb model for EH36 steel, focusing on fracture initiation modeling through different specimen types and hardening parameter determination using Swift-Voce functions. Both studies employ Abaqus and custom subroutines for numerical modeling, but the current approach emphasizes deep drawing fracture prediction using the Brozzo model, while their study focuses on steels and fracture initiation modeling through the Hosford-Coulomb model.

Notably, Watanabe *et al.* [45] employed stress-strain integration equations for accurate fracture initiation location determination in cold-forming processes. Similar to the current investigation, their study analyzes the Cockcroft & Latham model for fracture prediction, but with Brozzo model enhancement incorporating hydrostatic stresses—critical for high triaxial stress processes like deep drawing. Compared to classical criteria, this enables more accurate fracture prediction. Additionally, Zhang *et al.* [46] utilize the Continuum Damage Mechanics (CDM) model for ductile fracture prediction in single-point forming processes, considering stress state-dependent damage evolution. The current study applies the Brozzo model, emphasizing hydrostatic stress integration for improved deep drawing fracture prediction. Both approaches employ Abaqus/Explicit but differ in process types and damage models.

Thus, study results demonstrate that Brozzo criterion implementation in Abaqus accurately predicts failure initiation during deep drawing, confirming damage zone detection accuracy. Concurrently, UMAT modeling provides precise damage control during material deformation, establishing the Brozzo method as effective for failure prediction in complex processes like deep drawing.

4. Conclusion

This study provided a comparative evaluation of several ductile fracture criteria with the aim of identifying an appropriate modelling approach for deep drawing simulations. Among the models considered, the Brozzo criterion demonstrated a favourable compromise between predictive capability and numerical efficiency when applied to conditions involving large plastic deformation and complex stress states. The implementation of the Brozzo damage formulation within the Abaqus finite element framework through a user-defined material subroutine enabled reliable prediction of damage evolution and fracture initiation during the forming process. The numerical results highlight the ability of this approach to identify critical regions susceptible to failure, thereby enhancing the robustness of deep drawing simulations. From a practical standpoint, the proposed modelling strategy is well suited for integration into industrial forming analyses, where accurate fracture prediction is essential for process optimisation and quality improvement. While the approach entails a higher computational cost than simpler fracture criteria, its improved physical relevance justifies its use for applications requiring reliable failure assessment. Future work will focus on extending the experimental validation to a wider range of materials and forming conditions, as well as on incorporating additional effects such as temperature and strain rate, in order to further improve the predictive capability and applicability of the model.

References

[1] L.D. Giang, D.H. Tran, L. Q. Dũng, V.C. Nguyen, V.H. Nguyen, *Prediction of earing in deep drawing of the cylindrical cup of stainless steel SUS304 by numerical simulation*, J. Military Sci. Tech. 86 (2023) 129–136. https://doi.org/10.54939/1859-1043.j.mst.86.2023.129-136

[2] X.G. Hà, T.T. Nguyễn, V.A. Lê, *Numerical simulation of the springback of copper alloy thin sheets after the forming process*, Hong Duc Univ. J. Sci. 71(11) (2024) 5–14. https://doi.org/10.70117/hdujs.2.2024.734

[3] Vũ Bá Thành, *Uses an innovative phase field method to enhance the accuracy of damage simulation in typical structures*, Tạp Chí Khoa Học Công Nghệ Xây Dựng 18(4V) (2024) 122–136. https://doi.org/10.31814/stce.huce2024-18(4V)-10

[4] S. Laboubi, O. Boussaid, M. Zaaf, W. Ghennai, *Numerical investigation and experimental validation of Lemaitre ductile damage model for DC04 steel and application to deep drawing process*, Int. J. Adv. Manuf. Technol. 126 (2023) 2283–2294. https://doi.org/10.1007/s00170-023-11244-0

[5] X. Zhu, Z. Lv, J. Shuai, L. Shi, S. Yu, G. Xia, *Ductile fracture criterion parameter calibration and analysis: X80 pipe steel*, Pressure Vessels and Piping Conf. (2024). https://doi.org/10.1115/PVP2024-123037

[6] S. Dey, R. Kiran, *A Data-driven geometry-specific surrogate model for forecasting the load-displacement behavior until ductile fracture*, Int. J. Fract. 249 (2025) 31. https://doi.org/10.1007/s10704-025-00839-1

[7] H. Talebi-Ghadikolaee, H. Moslemi Naeini, E. Talebi Ghadikolaee, M.J. Mirnia, *Predictive modeling of damage evolution and ductile fracture in bending process*, Mater. Today Commun. 31 (2022) 103543. https://doi.org/10.1016/j.mtcomm.2022.103543

[8] H. Talebi-Ghadikolaee, H. Moslemi Naeini, M.J. Mirnia, M.A. Mirzai, H. Gorji, S. Alexandrov, *Ductile fracture prediction of AA6061-T6 in roll forming process*, Mech. Mater. 148 (2020) 103498. https://doi.org/10.1016/j.mechmat.2020.103498

[9] D. Wang, Z. Xu, Y. Han, F.A. Huang, *A ductile fracture model incorporating stress state effect*, Int. J. Mech. Sci. 241 (2022) 107965. https://doi.org/10.1016/j.ijmecsci.2022.107965

[10] Y. Guo, Y. Xie, D. Wang, L. Du, J. Zhao, *An improved damage-coupled viscoplastic model for predicting ductile fracture in aluminum alloy at high temperatures*, J. Mater. Process. Technol. 296 (2021) 117229. https://doi.org/10.1016/j.jmatprotec.2021.117229

[11] M. Kovzel, V. Kutzova, Regularities of the formation of structure, phase composition and tribological properties of heat-resistant chromium-nickel alloys Nikorin, In “Structural materials: Manufacture, properties, conditions of use: Collective monograph, Technology Center, Kharkiv (2023) 68–120”.

[12] V.Z. Kutsova, M.A. Kovzel, A.V. Grebeneva, A.S. Myrgorodskaya, *Structure, phases and alloying elements distribution of nikorim (high-temperature strength Ni-Cr alloy) in its cast form*, Metal. Mining Indust. 4(1) (2012) 40–44.

[13] D. Malecha, R. Albrecht, J. Lamb, S. Małecki, *The Influence of Lead Refining Method on the Dross Content in the Metal*, JOM 77(9) (2025) 6603–6619. https://doi.org/10.1007/s11837-025-07558-x

[14] V.Z. Kutsova, M.A. Kovzel, P.U. Shvets, A.V. Grebeneva, V.V. Prutchykova, *Structure, phase composition of supercooled austenite, and kinetics of its decomposition in perlite temperature range of chromium-manganese cast iron*, Metallofiz. Noveishie Tekhnol. 40(4) (2018) 551–560. https://doi.org/10.15407/mfint.40.04.0551

[15] O. Merkulov, R. Podolskyi, A. Kononenko, E. Safronova, E. Klemeshov, *Development of Promising Steels for Railway Rails of a New Generation Using Modeling of Phase-Structural Transformations*, Transact. Indian Inst. Met. 77(8) (2024) 1873–1889. https://doi.org/10.1007/s12666-024-03265-4

[16] O.I. Babachenko, G.A. Kononenko, R.V. Podolskyi, O.A. Safronova, O.L. Safronov, Z.A. Dementiev, *Study of correlation of chemical and phase composition and fracture toughness of railway wheel steel*, Mater. Sci. 60(1) (2024) 33–38. https://doi.org/10.1007/s11003-024-00847-x

[17] B.T. Ratov, V.A. Mechnik, N.A. Bondarenko, V.M. Kolodnitskyi, E.S. Gevorkyan, V.P. Nerubaskyi, A.G. Gusmanova, B.V. Fedorov, N.A. Kaldibaev, M.T. Arshidinova, V.G. Kulych, *Features of the Structure of the Diamond–(WC–Co)–ZrO_2 Composite Fracture Surface under Impact Loading*, J. Superhard Mater. 45(5) (2023) 348–359. https://doi.org/10.3103/S1063457623050088

[18] M.Y. Kharlamov, I.V. Krivtsun, V.N. Korzhyk, Y.V. Ryabovolyk, O.I. Demyanov, *Simulation of Motion, Heating, and Breakup of Molten Metal Droplets in the Plasma Jet at Plasma-Arc Spraying*, J. Therm. Spray Technol. 24(4) (2015) 659–670.

[19] S. Peleshenko, V. Korzhyk, O. Voitenko, V. Khaskin, V. Tkachuk, *Analysis of the current state of additive welding technologies for manufacturing volume metallic products (review)*, East-Eur. J. Enterp. Technol. 3(1-87) (2017) 42–52.

[20] S. Adjamskiy, G. Kononenko, R. Podolskyi, S. Baduk, *Studying the influence of orientation and layer thickness on the physico-mechanical properties of Co-Cr-Mo alloy manufactured by the SLM method*, Sci. Innov. 18(5) (2022) 85–94. https://doi.org/10.15407/scine18.05.085

[21] V.G. Piskunov, A.V. Marchuk, Ya.L. Il'chenko, *Free vibrations of thick layered cylindrical shells*, Mechan. Compos. Mater. 47(2) (2011) 177–184. https://doi.org/10.1007/s11029-011-9196-8

[22] V.V. Chygyryns'kyy, V.G. Shevchenko, I. Mamuzic, S.B. Belikov, *A new solution of the harmonic functions in the theory of elasticity*, Mater. Tehnol. 44(4) (2010) 219–222.

[23] L. Storozhenko, V. Butsky, O. Taranovsky, *Stability of compressed steel concrete composite tubular columns with centrifuged cores*, J. Construct. Steel Res. 46(1-3) (1998) 484. https://doi.org/10.1016/S0143-974X(98)80098-9

[24] V. Korzhyk, V. Khaskin, A. Grynyuk, O. Ganushchak, S. Peleshenko, O. Konoreva, O. Demianov, V. Shcheretskiy, N. Fialko, *Comparing Features In Metallurgical Interaction When Applying Different Techniques Of Arc And Plasma Surfacing Of*

Steel Wire On Titanium, East-Eur. J. Enterp. Technol. 4(12-112) (2021) 6–17.

[25] Y. Kononov, O. Lymar, *Stability of the coupled liquid-elastic bottom oscillations in a rectangular tank*, J. Theor. Appl. Mech. (Bulgaria) 52(2) (2022) 164–178. https://doi.org/10.55787/jtams.22.52.2.164

[26] N. Nikolov, D. Pashkouleva, A. Yanakieva, *Identification of mechanical characteristics of an amorphous metallic material*, Compt. Rend. L'Acad. Bulg. Sci. 66(1) (2013) 119–126. https://doi.org/10.7546/CR-2013-66-1-13101331-15

[27] D. Nedeva, *Preparation, properties, and application of titanium carbide coatings*, Zeitschr. Naturforsch. – Sec. A J. Phys. Sci. (2025). https://doi.org/10.1515/zna-2025-0152

[28] Z. Jia, L. Mu, B. Guan, L.-Y. Qian, Y. Zang, *Experimental and numerical study on ductile fracture prediction of aluminum alloy 6016-T6 sheets using a phenomenological model*, J. Mater. Engin. Perf. 31 (2021) 867-881. https://doi.org/10.1007/s11665-021-06248-4

[29] Y. Zhang, F. Shen, J. Zheng, S. Muenstermann, T. Li, W. Han, S. Huang, *Ductility prediction of HPDC aluminum alloy using a probabilistic ductile fracture model*, Theoret. Appl. Fract. Mech. 119 (2022) 103381. https://doi.org/10.1016/j.tafmec.2022.103381

[30] İ.T. Tandoğan, T. Yalcinkaya, *Development and implementation of a micromechanically motivated cohesive zone model for ductile fracture*, Int. J. Plasticity 158 (2022) 103427. https://doi.org/10.1016/j.ijplas.2022.103427

[31] G.Y. Akitarak, Ductile failure analysis during backward flow forming processes, Ankara: Middle East Technical University (2024).

[32] S. Choi, T. Park, H. Kim, B. Nam, B. Ye, D. Kim, *Ductile fracture prediction in thin-walled structures through a novel damage model*, Heliyon 10(23) (2024) e40849. https://doi.org/10.1016/j.heliyon.2024.e40849

[33] M. Khaboushani, A. Aminzadeh, A. Parvizi, *A novel estimation of tearing limit in deep drawing process based on strain energy; experimental characterization and numerical validation*, Int. J. Adv. Manufact. Tech. 123 (2022) 927-942. https://doi.org/10.1007/s00170-022-10158-7

[34] L. Ben Said, M. Allouch, M. Wali, F. Dammak, *Numerical formulation of anisotropic elastoplastic behavior coupled with damage model in forming processes*, Mathematics 11(1) (2023) 204. https://doi.org/10.3390/math11010204

[35] J.D. Clayton, Analysis of adiabatic shear coupled to ductile fracture and melting in viscoplastic metals, arXiv (2025). https://doi.org/10.48550/arXiv.2502.10625

[36] F. Van den Abeele, Parameter calibration for continuum damage mechanics models to simulate ductile fracture of high strength pipeline steels, ASME 2019 38th Int. Conf. Ocean, Offshore Arctic Engin. (2019). https://doi.org/10.1115/OMAE2019-96316

[37] F. Hosseini Mansoub, A. Basti, A. Darvizeh, A. Zajkani, *Stress-based forming limit diagrams (SFLD) considering strain rate effect and ductile damage phenomenon*, Int. J. Mater. Res.

111(2) (2020) 136-145.
https://doi.org/10.3139/146.111856

[38] R. Ma, W. Sun, G. Tong, *Phase-field model for ductile fracture in the stress resultant geometrically exact shell*, Int. J. Num. Methods Engin. 125(13) (2024) e7462.
https://doi.org/10.1002/nme.7462

[39] S. Basak, S. Panda, *Use of uncoupled ductile damage models for fracture forming limit prediction during two-stage forming of aluminum sheet material*, J. Manufact. Processes 97 (2023) 185-199.
https://doi.org/10.1016/j.jmapro.2023.04.042

[40] M. Ganjiani, *A damage model for predicting ductile fracture with considering the dependency on stress triaxiality and lode angle*, Europ. J. Mech. – A/Solids 84(4) (2020) 104048.
https://doi.org/10.1016/j.euromechsol.2020.104048

[41] P. Wu, Y. Lou, *Stress-based fracture model to describe ductile fracture behavior in various stress states*, Fatigue & Fracture Engin. Materials & Struc. 48(3) (2024) 1200-1214.
https://doi.org/10.1111/ffe.14548

[42] S. Fagerhøi, A.K. Bergsbakken, Abaqus FEA with concrete damaged plasticity and its feasibility in recreating laboratory experiments: A numerical analysis and sensitivity study, Oslo: Oslo Metropolitan University (2023).

[43] A. Aksen, B. Şener, E. Esener, M. Firat, *Evaluation of ductile fracture criteria in combination with a homogenous polynomial yield function for edge splitting damage of DP steels*, Materials Test. 65(6) (2023) 824-843.
https://doi.org/10.1515/mt-2022-0359

[44] S.-J. Park, K. Lee, J.H. Seo, J. Choung, *Ductile fracture prediction of EH36 grade steel based on hosford-coulomb model*, Ships Offshore Struct. 14(1) (2019) 219-230.
https://doi.org/10.1080/17445302.2019.1565300

[45] A. Watanabe, K. Hayakawa, S. Fujikawa, *An anisotropic damage model for prediction of ductile fracture during cold-forging*, Metals 12(11) (2022) 1823.
https://doi.org/10.3390/met12111823

[46] K. Zhang, Z.M. Yue, C.J. Su, R. Wang, H. Badreddine, *Modelling of ductile damage in single point incremental forming process using enhanced CDM model*, IOP Conf. Ser. Mat. Sci. Engin. 1270 (2022) 012022.
https://doi.org/10.1088/1757-899X/1270/1/012022